Electronic supplementary information (ESI)

Ionic Liquid-Directed Synthesis of Au—AgBr Janus Nanoparticles via Digestive Ripening and Solvated Metal Atom Dispersion

Saibalendu Sarkar;[a] and Balaji R. Jagirdar*[a]

[a] *Department of Inorganic and Physical Chemistry, Indian Institute of Science, Bangalore 560012, India.*

ORCID ID: JAGIRDAR: https://orcid.org/0000-0002-0048-2252; SARKAR: https://orcid.org/0009-0002-0416-374X

Email: jagirdar@iisc.ac.in

1. Annexure S1

1.1 Materials: Gold foil (99.95%) and silver foil (99.99%) were purchased from Arora-Matthey Limited (Kolkata, India). 1-Butylimidazole (99%), 1-octadecyl bromide (99.5%), chloroauric acid ($HAuCl_4$, 99%), and silver nitrate ($AgNO_3$, 98%) were procured from Sigma-Aldrich. Lithium bis(trifluoromethanesulfonyl)imide (98%) was purchased from TCI Chemicals. HPLC-grade dichloromethane, toluene, acetonitrile, and ethyl acetate were procured from S. D. Fine Chemicals Limited, India, and used without further purification. Toluene was dried over sodium-benzophenone and then distilled and degassed by several freeze-pump-thaw cycles before use. Sodium borohydride ($NaBH_4$, 98%) was purchased from Spectrochem Private Limited, India.

1.2 Instrumentation: Optical absorption spectral measurements were carried out at room temperature using a Shimadzu UV-2600 UV—vis—near—IR spectrophotometer. The microscopic (TEM) analysis of the samples was carried out using a JEOL JEM-2100F field emission transmission electron microscope operating at an accelerating voltage of 200 kV. The samples were prepared on Formvar based carbon coated copper grids by slow evaporation of 1—2 μL of the diluted colloids and further drying under a lamp. The particle size distribution of the samples was calculated by measuring the size of a minimum of 250 particles imaged from different regions of the TEM grid using ImageJ software. High-resolution (HR) TEM and selected-area electron diffraction (SAED) pattern analysis were performed with the help of Digital Micrograph software. High-angle annular dark-field (HAADF) along with scanning

transmission electron microscopy (STEM) and energy dispersive X-ray spectroscopy (EDS) were carried out using a ThermoFischer Talos F200 S instrument at an operating voltage of 200 kV. X-ray photoelectron spectroscopy (XPS) data were obtained using a ThermoFischer Scientific K-alpha instrument with Al Kα as X-ray source. The samples for XPS analysis were prepared by drop-casting a concentrated colloid on silicon wafers. The peak fitting of the individual core levels was done using CASAXPS software with a Shirley type background. ^{1}H NMR spectral measurements were carried out using a Bruker Avance II 400 MHz instrument. Powder X-ray diffraction (PXRD) data were collected on a Bruker D8 Advance X-ray diffractometer equipped with a Cu Kα (0.154 nm) radiation source. High Resolution Mass Spectrometric (HRMS) analysis was carried out in Waters Xevo G3 QTOF-HRMS instrument.

1.3 Synthesis of ionic liquids (ILs)

1.3.1 Synthesis of 1-butyl-3-octadecylimidazolium bromide [C_{18}BIm]Br: The [C_{18}BIm]Br ionic liquid was prepared according to a previous report via a bimolecular nucleophilic substitution reaction (S_N2) in a solvent under reflux conditions.[1] 1-Butylimidazole [1.0 g, 8 mmol], 1-octadecylbromide [3.0 g, 8 mmol], and acetonitrile [15 mL] were refluxed in a round bottom flask at 348 K for 72 h under an inert atmosphere. The resultant hot reaction mixture was then poured drop-wise onto a 100 mL cold (243 K) ethylacetate solvent for rapid crystallization. The colorless solid was washed using ethyl acetate a few times. After filtering, the solid was dried under vacuum at 10^{-6} bar and 343 K for 72 h before use. [C_{18}BIm]Br was characterized using ^{1}H NMR, ^{13}C NMR spectroscopy, and mass spectrometry. Isolated yield is 76%. The melting point of the ionic liquid is 40-42 ^{o}C. The solubility of [C_{18}BIm]Br in water is 11 mg/mL of water at room temperature.

^{1}H NMR ($CDCl_3$, 298 K, 400 MHz): δ 10.45 (s, 1H, -N-C<u>H</u>-N-), 7.52 (d, 1H, -N-C<u>H</u>-CH-), 7.46 (d, 1H, -CH-C<u>H</u>-N-), 4.33 (t, 2H, -CH_2-C<u>H_2</u>-N-), 4.30 (t, 2H, -N-C<u>H_2</u>-CH_2-), 1.87 (q, 4H, -CH_2-C<u>H_2</u>-CH_2-N-), 1.20 (br, 34H, -CH_2-CH_2-$(CH_2)_{15}$-CH_3 + CH_3-C<u>H_2</u>-CH_2-CH_2-N), 0.91 (t, 3H, C<u>H_3</u>-CH_2-CH_2-), 0.82 (t, 3H, -CH_2-$(CH_2)_{16}$-C<u>H_3</u>)

^{13}C NMR ($CDCl_3$, 298 K, 100 MHz): δ 137.0, 122.2, 122.0, 50.0, 49.7, 50.2, 32.2, 31.8, 30.9, 30.3, 29.6, 29.4, 29.3, 28.9, 26.2, 22.6, 19.4, 14.0, 13.4

ESI-MS (+ve ion) (m/z): 377.37

ESI-MS (-ve ion) (m/z): 78.91 (^{79}Br), 80.91 (^{81}Br)

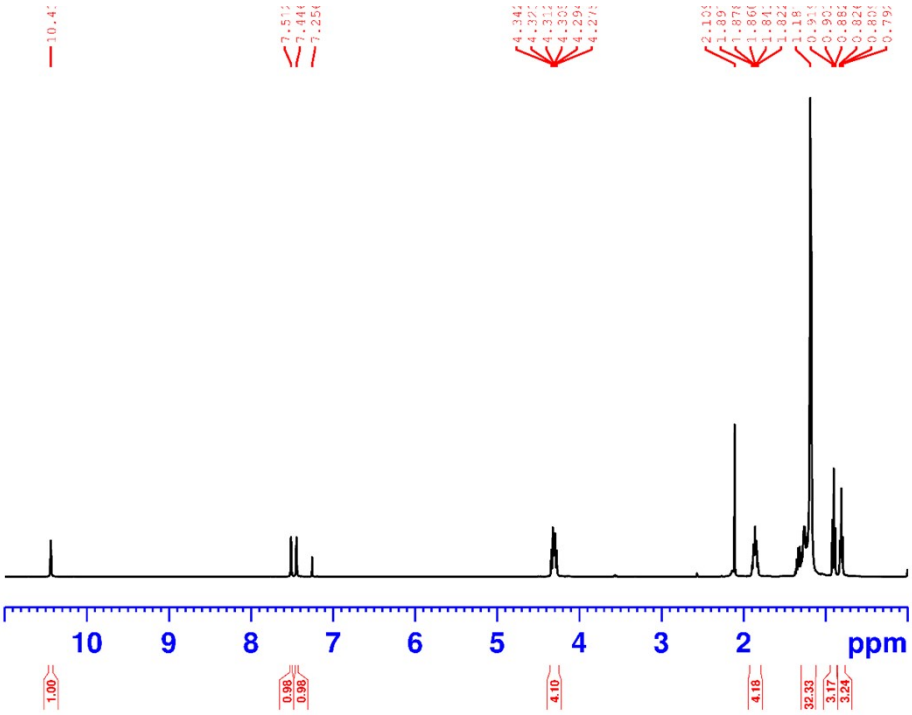

Fig. S1 ^{1}H NMR spectrum of [C_{18}Bim]Br ($CDCl_3$, 400 MHz, 298 K)

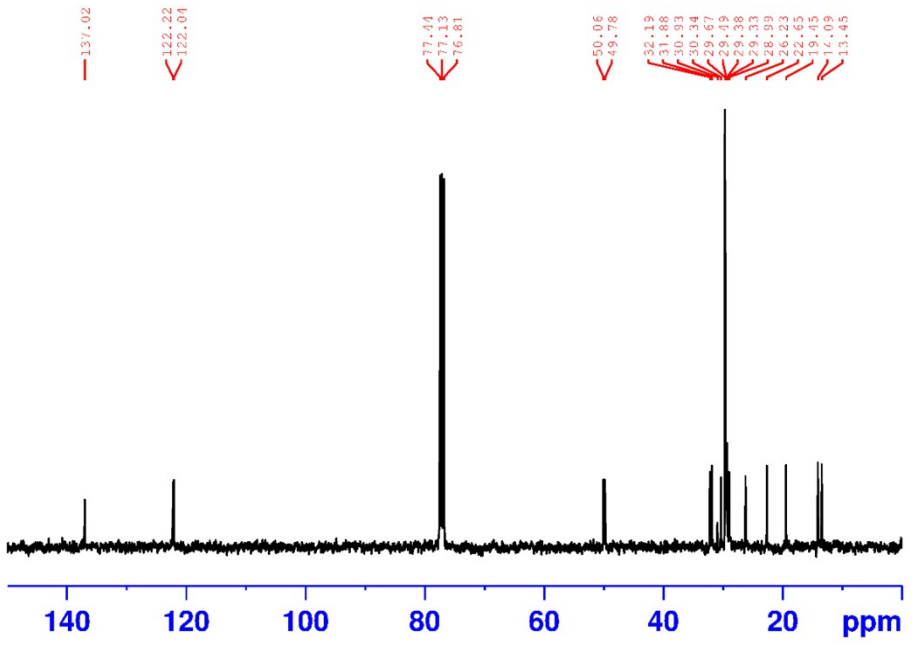

Fig. S2 ^{13}C NMR spectrum of [C_{18}Bim]Br ($CDCl_3$, 100 MHz, 298 K)

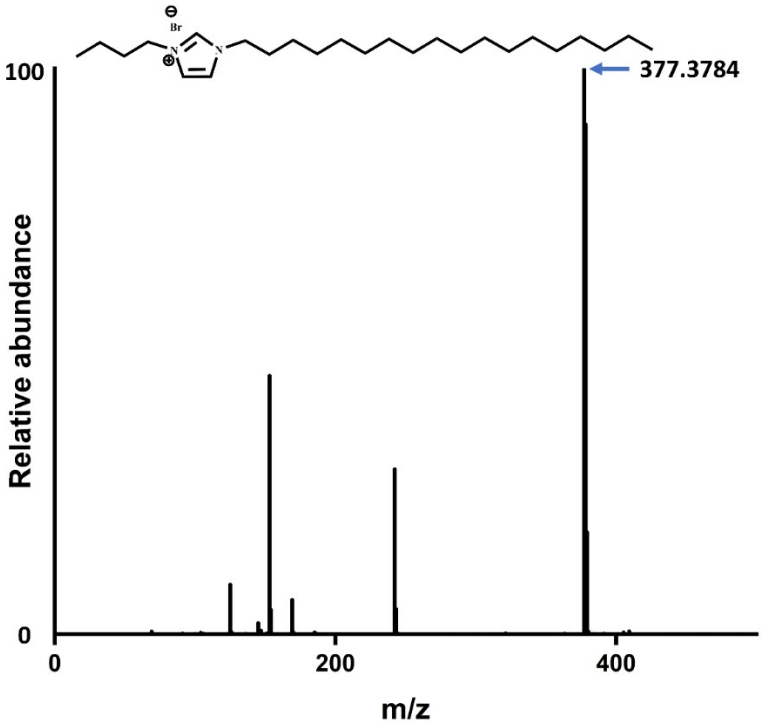

Fig. S3 (+ve) ion mass spectrum of [C_{18}Bim]Br

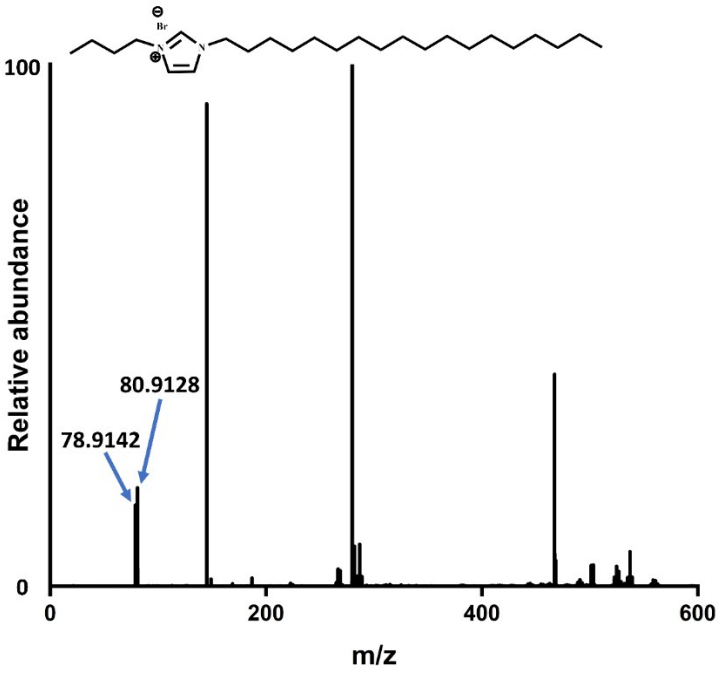

Fig. S4 (-ve) ion mass spectrum of [C_{18}Bim]Br

1.3.2 Synthesis of 1-Butyl-3-octadecylimidazolium bis(trifluoromethylsulfonyl)imide [C_{18}BIm]NTf_2: The bis(trifluoromethylsulfonyl)imide (NTf_2) IL was prepared from [C_{18}BIm]Br by an anion metathesis reaction reported previously.[1] 1-Butyl-3-octadecylimidazolium bromide [1.0 g, 2.18 mmol] was dissolved in 10 mL of CH_2Cl_2, and then it was added to a solution of lithium bis(trifluoromethyl sulfonyl)imide [0.625 g, 8.6 mmol] in 5 mL of deionized water. The mixture was stirred for a day at room temperature under an inert atmosphere. The dichloromethane phase was separated using a separating funnel and repeatedly washed with water to remove the bromide anion. The solvent was removed in vacuo, and the resulting colorless viscous liquid was dried at 343 K under vacuum at 10^{-6} bar for at least 72 h before use. [C_{18}BIm]NTf_2 was characterized using ^{1}H NMR, ^{13}C NMR, and ^{19}F NMR spectroscopy as well as mass spectrometry. Isolated yield is 64%. The melting point of the ionic liquid is 47-49 ^{o}C. The solubility of [C_{18}BIm]NTf_2 in water is 7 mg/mL of water at room temperature. Due to the sparing solubility of [C_{18}BIm]NTf_2 in water, the net yield of the product was affected during the repeated washing of the ionic liquid solution in CH_2Cl_2 with water. After each wash with water, the presence of Br^- ion was monitored using an $AgNO_3$ solution, and the washing cycle continued till no presence of AgBr was observed in the aqueous phase.

^{1}H NMR ($CDCl_3$, 298 K, 400 MHz): δ 8.82 (s, 1H, -N-C<u>H</u>-N-), 7.34 (d, 1H, -N-C<u>H</u>-CH-), 7.32 (d, 1H, -CH-C<u>H</u>-N-), 4.18 (t, 2H, -CH_2-C<u>H_2</u>-N-), 4.17 (t, 2H, -N-C<u>H_2</u>-CH_2-), 1.85 (q, 4H, -CH_2-C<u>H_2</u>-CH_2-N-), 1.24 (br, 34H, -CH_2-CH_2-$(CH_2)_{15}$-CH_3 + CH_3-C<u>H_2</u>-CH_2-CH_2-N), 0.95 (t, 3H, C<u>H_3</u>-CH_2-CH_2-), 0.87 (t, 3H, -CH_2-$(CH_2)_{16}$-C<u>H_3</u>)

^{13}C NMR ($CDCl_3$, 298 K, 100 MHz): δ 135.4, 123.4, 123.3, 121.4, 118.3, 50.2, 49.9, 32.0, 31.9, 30.9, 30.1, 29.7, 29.6, 29.4, 29.3, 28.8, 26.1, 22.7, 19.3, 14.2, 12.1

^{19}F NMR ($CDCl_3$, 298 K, 376 MHz): δ -79.0

ESI-MS (+ve ion) (m/z): 377.37

ESI-MS (-ve ion) (m/z): 279.90

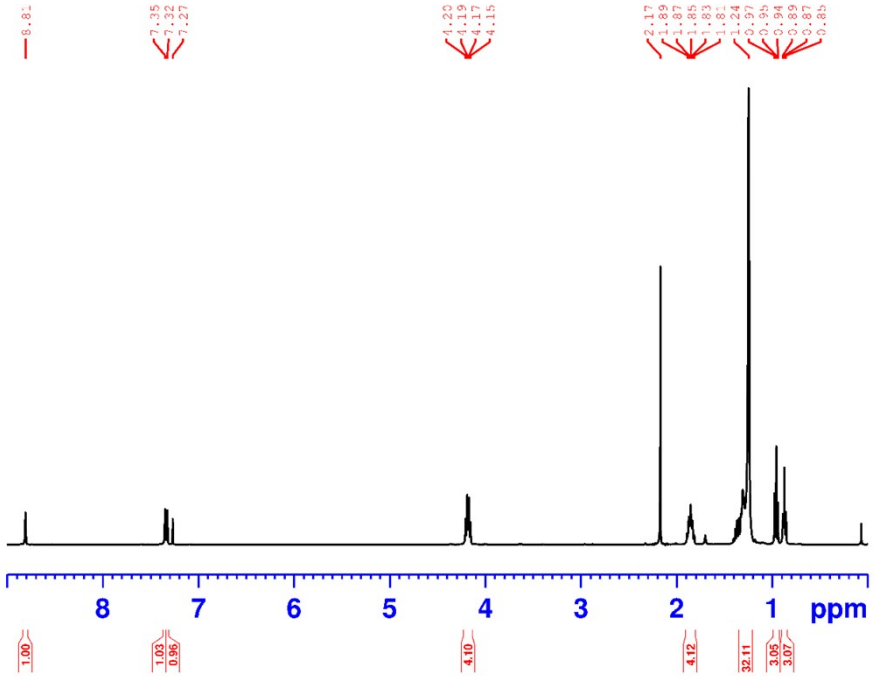

Fig. S5 ^{1}H NMR spectrum of $[C_{18}Bim]NTf_2$ ($CDCl_3$, 400 MHz, 298 K)

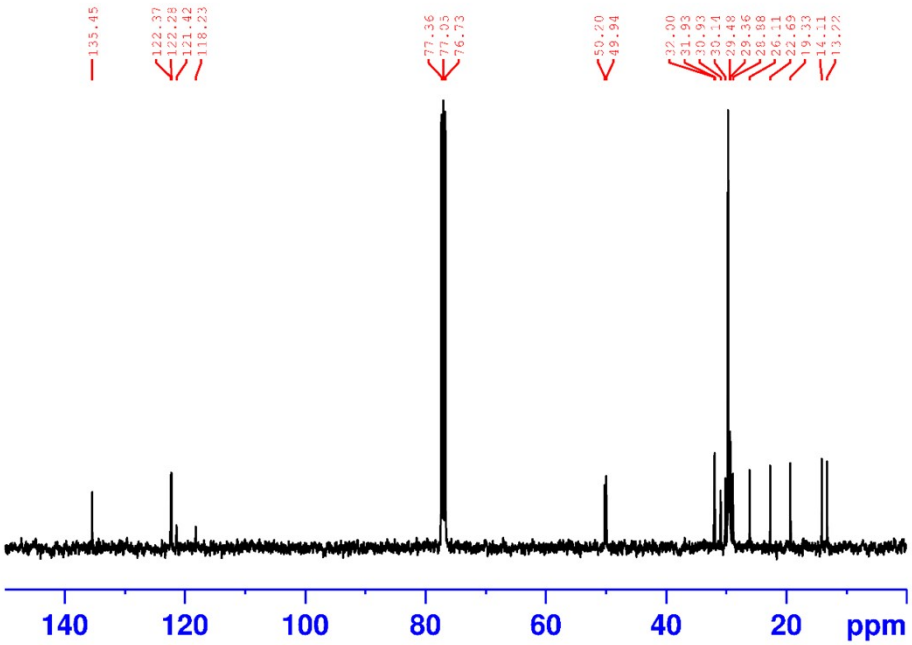

Fig. S6 ^{13}C NMR spectrum of $[C_{18}Bim]NTf_2$ ($CDCl_3$, 100 MHz, 298 K)

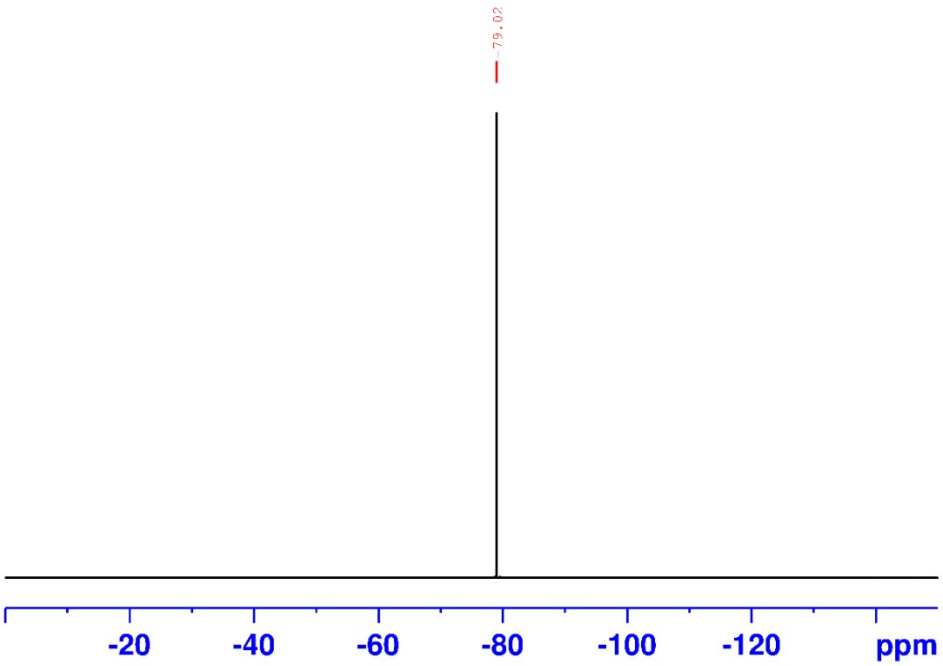

Fig. S7 ^{19}F NMR spectrum of $[C_{18}Bim]NTf_2$ ($CDCl_3$, 376 MHz, 298 K)

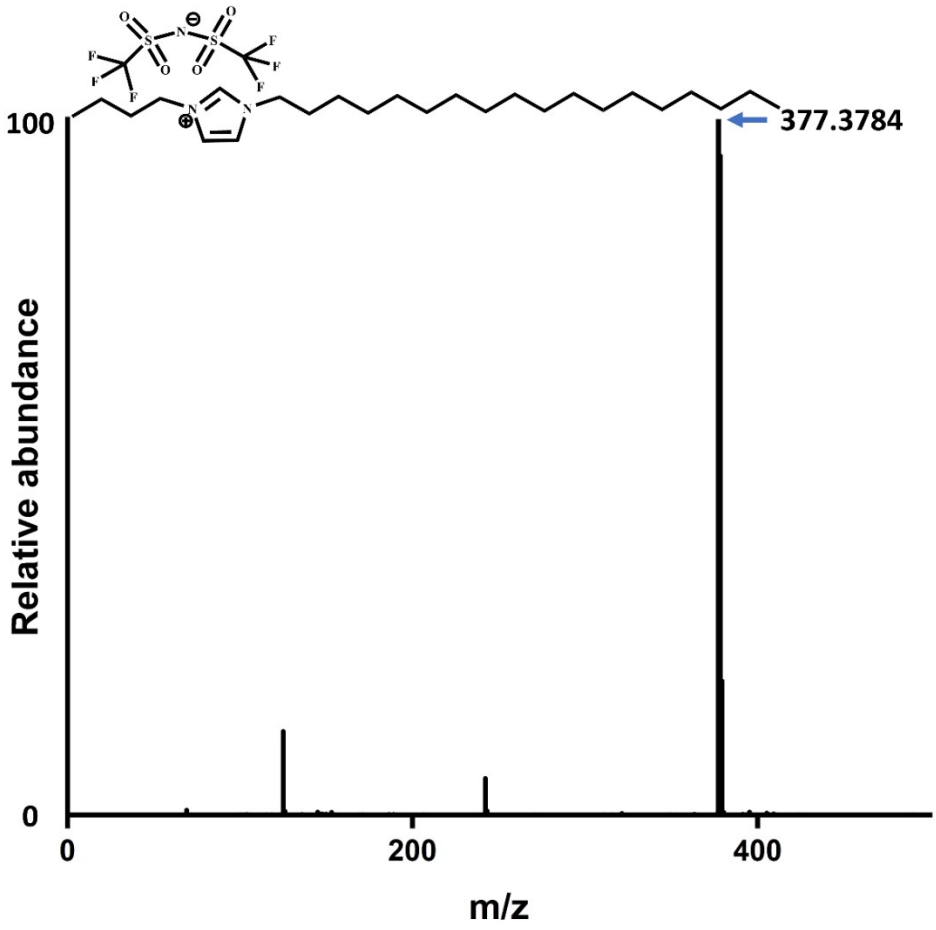

Fig. S8 (+ve) ion mass spectrum of $[C_{18}Bim]NTf_2$

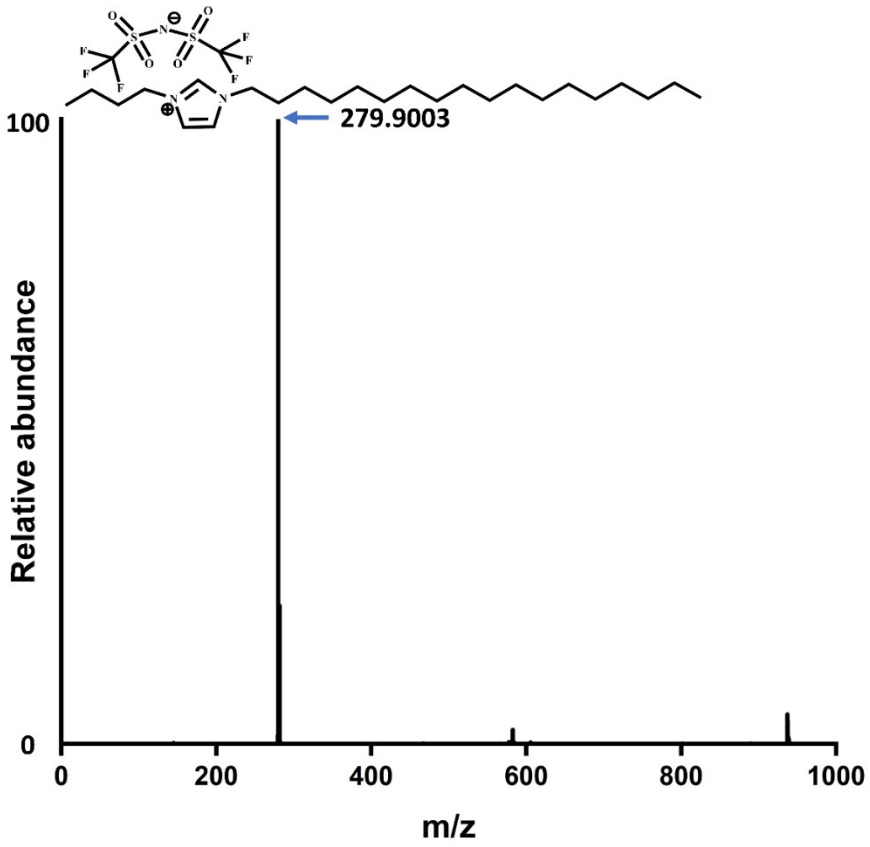

Fig. S9 (-ve) ion mass spectrum of $[C_{18}Bim]NTf_2$

1.4 As-prepared colloids by the solvated metal atom dispersion (SMAD) method: Metal nanoparticles solvated by toluene, were prepared by the solvated metal atom dispersion (SMAD) method.[2] Typically, high-purity metal (>99.9%) foil was placed in an alumina-coated tungsten crucible connected to two water-cooled copper electrodes. A Schlenk tube containing dried, distilled, and degassed toluene was attached to the SMAD reactor (3 L, thick-walled, cylindrically shaped glass vessel) at the top through a bridge-head. The entire setup was then evacuated to about 1×10^{-3} mbar. The crucible was resistively heated, which led to the vaporization of the metal. The metal atoms formed were co-condensed with solvent vapor on the walls of the reactor immersed in a liquid N_2 dewar. After the completion of co-condensation, the frozen matrix of metal atoms and solvent molecules was allowed to warm up to room temperature. The as-prepared colloid was stored in a Schlenk tube under an argon atmosphere. These as-prepared colloids were found to be polydisperse in nature.

1.5 Preparation of ionic liquid (IL) capped colloids via solvated metal atom dispersion (SMAD) method and digestive ripening (DR): The colloidal metal nanoparticles prepared

by the SMAD method were subjected to digestive ripening process. In this process, the as-prepared colloid was taken in a 100 mL round-bottom Schlenk flask containing a solution of IL in toluene. The molar ratio of metal to IL, as well as the molar ratios between Ag and Au, were varied. Digestive ripening was carried out at an ambient temperature, and the mixture was vigorously stirred under an argon atmosphere. The experiment was continued for up to 1 h in each case. Sampling for UV—visible spectroscopy and transmission electron microscopy was done for the as-prepared and final colloids. Throughout this work, different colloids were labeled as per the molar ratio between Ag and Au; e.g., if the molar ratio between Ag and Au is 2:1, the colloid was labeled Ag_2Au.

2. Annexure S2

2.1 Preparation of different bimetallic Ag-Au colloids by co-evaporation via the solvated metal atom dispersion (SMAD) method and digestive ripening (DR) in ionic liquid (IL)

Ag and Au metal foils were placed together in a tungsten crucible for co-evaporation of metals in SMAD. The crucible was resistively heated, which led to the vaporization of the metals while maintaining the pressure of the reactor at 1×10^{-3} mbar. Both the metal atoms formed were co-condensed with toluene vapor on the walls of the reactor immersed in a liquid N_2 dewar. After the completion of co-condensation, the frozen matrix of metal atoms and toluene molecules was allowed to warm up to room temperature. The as-prepared colloid was subjected to digestive ripening at ambient temperature under an argon atmosphere for 1 h in ionic liquid in toluene. The molar ratio between total metal and IL was varied along with Ag and Au ratios to prepare different colloids as summarized in Table S1.

Table S1: Different Ag-Au bimetallic colloids in various metal and ionic liquid ratios.

Colloid	Ionic liquid	Content of Ag	Content of Au	Ag:Au molar ratio	Metal:Ionic liquid molar ratio
AgAu in low IL concentration	$[C_{18}BIm]Br$ (42 mg, 0.092 mmol)	Ag (25 mg, 0.231 mmol)	Au (45 mg, 0.228 mmol)	1:1	1:0.2
Ag_2Au in low IL concentration	$[C_{18}BIm]Br$ (38 mg, 0.083 mmol)	Ag (30 mg, 0.278 mmol)	Au (27 mg, 0.137 mmol)	2:1	1:0.2
$AgAu_2$ in low IL	$[C_{18}BIm]Br$	Ag (20 mg,	Au (73 mg,	1:2	1:0.2

concentration	(50 mg, 0.111 mmol)	0.185 mmol)	0.370 mmol)		
Ag_5Au in low IL concentration	$[C_{18}BIm]Br$ (56 mg, 0.122 mmol)	Ag (56 mg, 0.519 mmol)	Au (20 mg, 0.101 mmol)	5:1	1:0.2
AgAu in moderate IL concentration	$[C_{18}BIm]Br$ (195 mg, 0.426 mmol)	Ag (23 mg, 0.213 mmol)	Au (42 mg, 0.213 mmol)	1:1	1:1
AgAu in high IL concentration	$[C_{18}BIm]Br$ (2280 mg, 4.98 mmol)	Ag (27 mg, 0.250 mmol)	Au (49 mg, 0.248 mmol)	1:1	1:10
AgAu in low IL concentration	$[C_{18}BIm]NTf_2$ (53 mg, 0.092 mmol)	Ag (25 mg, 0.231 mmol)	Au (47 mg, 0.231mmol)	1:1	1:0.2

2.2 Preparation of bimetallic Ag-Au colloids by step-wise addition via the solvated metal atom dispersion (SMAD) method and digestive ripening (DR) in ionic liquid (IL): Au (45 mg, 0.228 mmol) foil was placed in a tungsten crucible, evaporated, and co-condensed with toluene solvent in a SMAD experiment. The as-prepared colloid obtained has a concentration of 1.1 mg/mL of the metal. The ionic liquid $[C_{18}BIm]Br$ (42 mg, 0.092 mmol) was added to this colloid in a metal to ionic liquid ratio of 1:0.4. The colloid was then allowed to stir for 30 min and kept idle for 72 h. In the next step, after 72 h, an as-prepared Ag (25 mg, 0.231 mmol) colloid in toluene prepared by SMAD experiment was added to the Au seed colloid and stirred for 60 min. The total metal to IL molar ratio was 5.

2.3 Preparation of bimetallic Ag-Au colloids by chemical reduction: $HAuCl_4$ solution (1 mL of 30 mM) was mixed with 0.5 mL of 60 mM $AgNO_3$ and stirred for 15 min at room temperature. To this solution, 10 mL of dichloromethane solution of $[C_{18}BIm]Br$ (1.2 mM) was added and stirred until the metal ions got transferred from the aqueous to the organic phase. This was confirmed by the disappearance of color in the aqueous phase and development of an intense yellow color in the organic phase. Ice-cooled $NaBH_4$ solution (5 mL of 12 mM) was added to the mixture drop-wise and stirred for 15 min at ambient temperature. The colloid in dichloromethane was isolated by extraction of the organic phase. The total metal to IL molar ratio was 5.

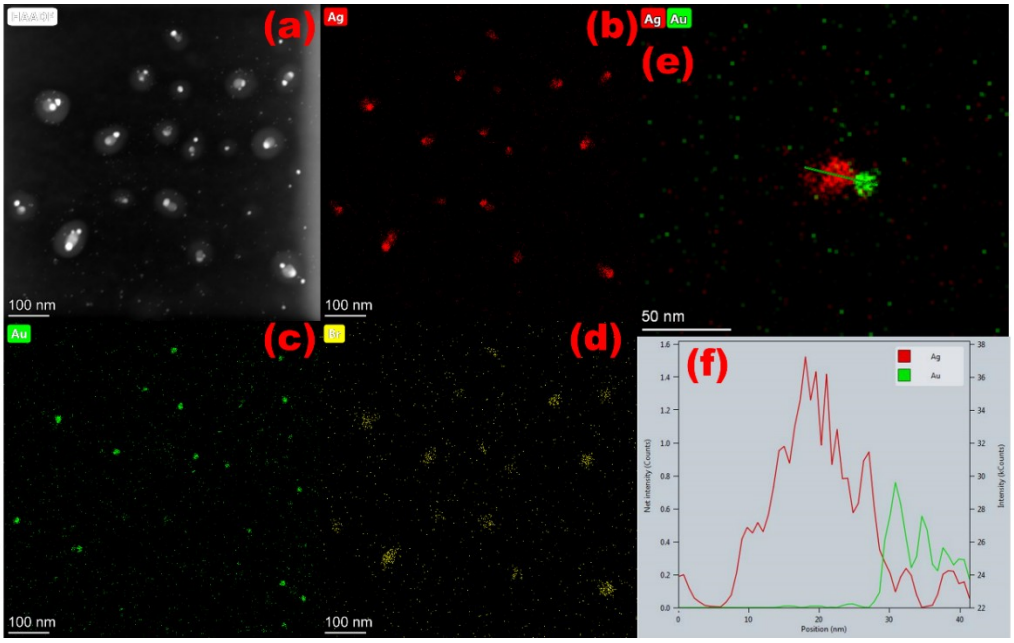

Fig. S10 (a) HAADF-STEM image, (b-d) STEM-EDS mapping, and (e,f) line scan profile of Au—AgBr Janus NPs in $AgAu_2$ colloid.

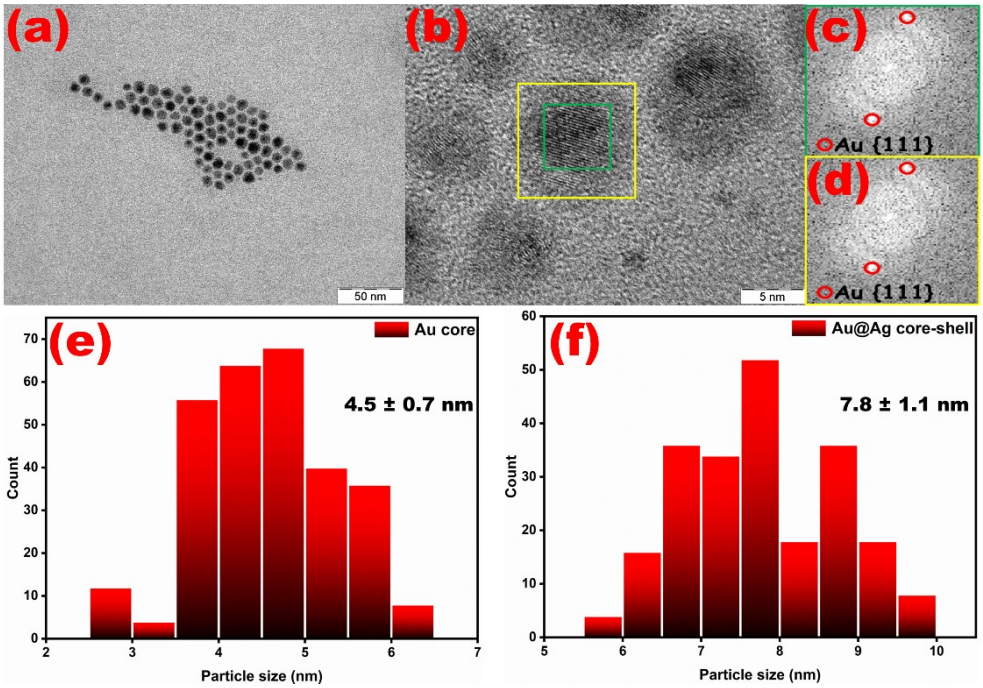

Fig. S11 (a) BFTEM and (b) HRTEM micrograph of micrographs of Au@Ag core-shell NPs in Ag_2Au colloid. (c,d) FFT pattern of the marked area. Particle size distribution of (e) Au and (f) Au@Ag core-shell particles in the Ag_2Au colloid.

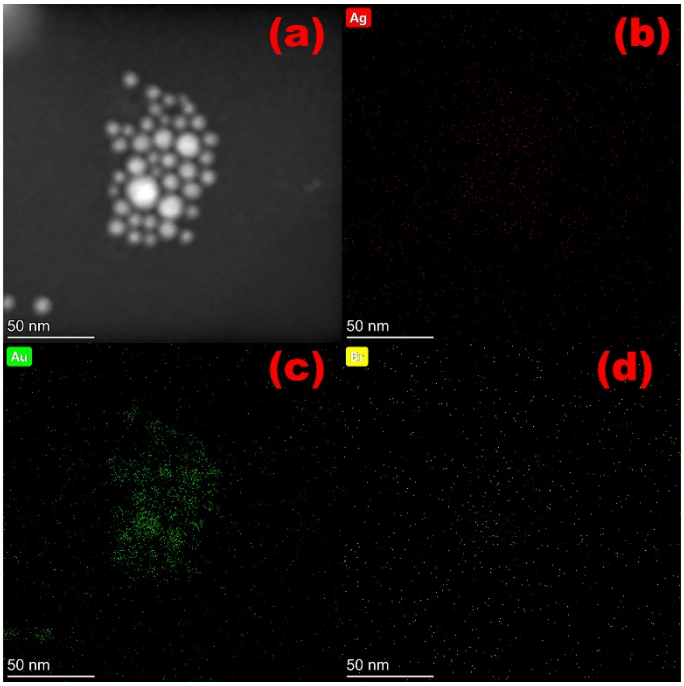

Fig. S12 (a) HAADF-STEM image, and (b-d) STEM-EDS mapping of partial AgAu alloy NPs in $AgAu_2$ colloid.

Table S2. Particle yields in different Ag-Au colloids.

Precursor Ag:Au molar ratio	Metal to ionic liquid molar ratio	Primary shape	Core-shell yield (%)	Janus yield (%)
2:1	5	Janus	15	55
1:1	5	Janus	0	85
1:2	5	Alloy	0	0

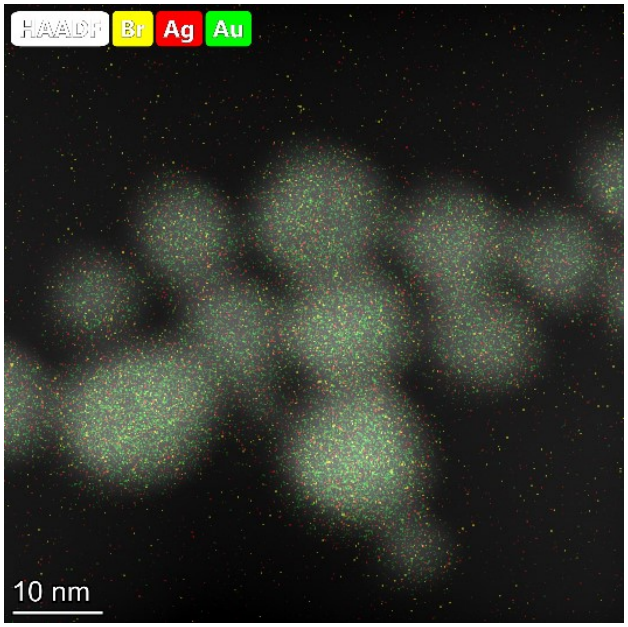

Fig. S13 HAADF-STEM-EDS mapping of connected spherical AgAu alloy NPs of step-wise addition preparation of AgAu colloid at 15 min reaction time.

Table S3. XPS binding energy peaks of Ag, Au, and Br in different colloids.

Sample	Elements	Components	Assignments	Binding Energy (eV)
Ag_2Au	Ag	Ag $3d_{5/2}^0$	---	---
		Ag $3d_{5/2}^+$	Ag (I) in AgBr [3]	367.8
		Ag $3d_{3/2}^0$	---	---
		Ag $3d_{3/2}^+$	Ag (I) in AgBr [3]	373.8
	Au	Au $4f_{7/2}^0$	Au (0) in Au–AgBr Janus[4]	84.4
		Au $4f_{7/2}^+$	Au (I) in IL[1]	85.1
		Au $4f_{5/2}^0$	Au (0) in Au–AgBr Janus[4]	87.5
		Au $4f_{5/2}^+$	Au (I) in IL[1]	88.7
	Br	Br $3d_{5/2}^-$	Bromide in AgBr[3]	68.0
		Br $3d_{3/2}^-$	Bromide in AgBr[3]	69.1

AgAu	Ag	Ag $3d_{5/2}^{0}$	---	---
		Ag $3d_{5/2}^{+}$	Ag (I) in AgBr[3]	367.6
		Ag $3d_{3/2}^{0}$	---	---
		Ag $3d_{3/2}^{+}$	Ag (I) in AgBr[3]	373.6
	Au	Au $4f_{7/2}^{0}$	Au (0) in Au–AgBr Janus[4]	83.8
		Au $4f_{7/2}^{+}$	Au (I) in IL[1]	85.2
		Au $4f_{5/2}^{0}$	Au (0) in Au–AgBr Janus[4]	87.2
		Au $4f_{5/2}^{+}$	Au (I) in IL[1]	88.9
	Br	Br $3d_{5/2}^{-}$	Bromide in AgBr[3]	67.8
		Br $3d_{3/2}^{-}$	Bromide in AgBr[3]	68.8
$AgAu_2$	Ag	Ag $3d_{5/2}^{0}$	Ag (0) in AgAu alloy[5]	368.5
		Ag $3d_{5/2}^{+}$	Ag (I) in IL[6]	367.6
		Ag $3d_{3/2}^{0}$	Ag (0) in AgAu alloy[5]	374.5
		Ag $3d_{3/2}^{+}$	Ag (I) in IL[6]	373.6
	Au	Au $4f_{7/2}^{0}$	Au (0) in AgAu alloy[5]	83.6
		Au $4f_{7/2}^{+}$	Au (I) in IL[1]	85.1
		Au $4f_{5/2}^{0}$	Au (0) in AgAu alloy[5]	87.3
		Au $4f_{5/2}^{+}$	Au (I) in IL[1]	88.8
	Br	Br $3d_{5/2}^{-}$	Bromide in ionic liquid[1]	68.2
		Br $3d_{3/2}^{-}$	Bromide in ionic liquid[1]	69.3

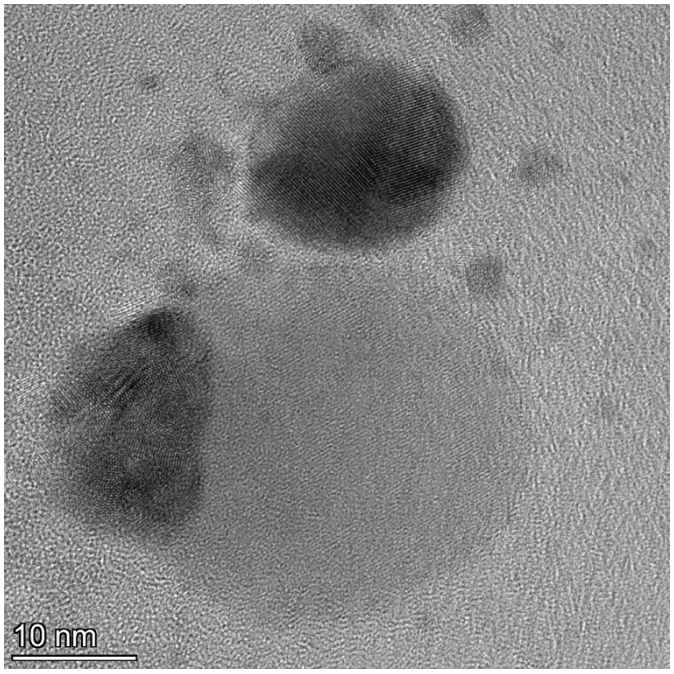

Fig. S14 HRTEM micrographs of an Au—AgBr Janus nanoparticles showing polycrystalline Au and monocrystalline AgBr components.

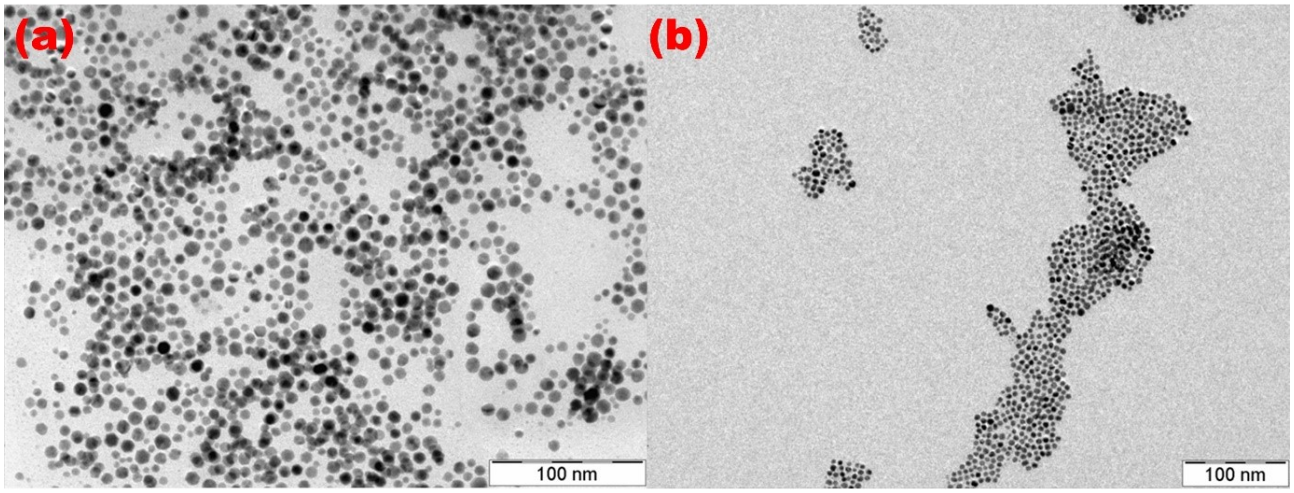

Fig. S15 BFTEM micrographs of (a) Au NPs at 30 min and (b) Ag NPs at 15 min in low concentration of IL (M:IL = 1:0.2) after ripening.

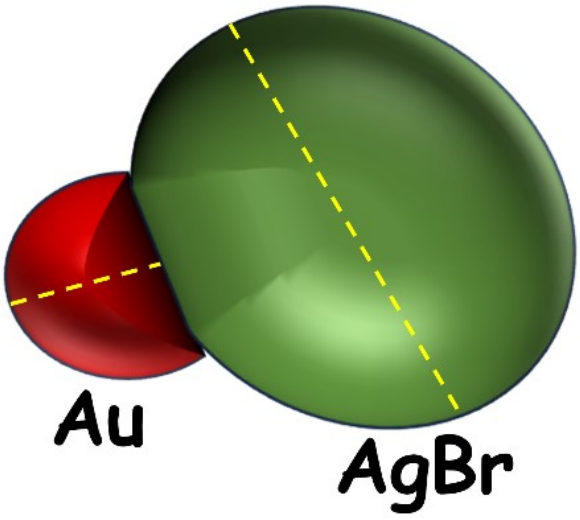

Fig. S16 Yellow dashed-line showing the length used to calculate the particle size distribution plots for Au and AgBr components in each Au–AgBr JNPs.

REFERENCES

1 S. Sarkar and B. R. Jagirdar, *Langmuir*, 2024, **40**, 7620–7631. https://doi.org/10.1021/acs.langmuir.4c00284

2 S. Stoeva, K. J. Klabunde, C. M. Sorensen and I. Dragieva, *J. Am. Chem. Soc.*, 2002, **124**, 2305–2311. https://doi.org/10.1021/ja012076g

3 H.Wang, X. Lang, J. Gao, W. Liu, D. Wu, Y. Wu, L. Guo and J. Li, *Chem. - Eur. J.*, 2012, **18**, 4620–4626. https://doi.org/10.1002/chem.201102694

4 R. Takahashi, M. Fujishima, H. Tada and T. Soejima, *ChemNanoMat*, 2020, **6**, 1485–1495. https://doi.org/10.1002/cnma.202000438

5 S. Malathi, T. Ezhilarasu, T. Abiraman and S. Balasubramanian, *Carbohydr. Polym.*, 2014, **111**, 734–743. https://doi.org/10.1016/j.carbpol.2014.04.105

6 H. Park, S. A. Hira, N. Muthuchamy, S. Park and K. H. Park, *Nanomaterials and Nanotechnology*, 2019, **9**. https://doi.org/10.1177/1847980419836500